Title

Changes in contaminant bioaccumulation and biochemical responses of *Carcinus maenas* in response to ecosystem restoration measures

V.H. Oliveira [1*], B. Marques [1], D. Crespo [2], A. Carvalhais [2], M. Dolbeth [3], A.I. Sousa [1], A.I. Lillebø [1], M. Pacheco [2], M.E. Pereira [4], C.L. Mieiro [2‡], J.P. Coelho [1‡]

[1] ECOMARE, CESAM - Centre for Environmental and Marine Studies, Department of Biology, University of Aveiro, Estrada do Porto de Pesca Costeira, 3830-565 Gafanha da Nazaré, Portugal;
[2] CESAM - Centre for Environmental and Marine Studies, Department of Biology, University of Aveiro, Campus Universitário de Santiago, 3810-193 Aveiro, Portugal;
[3] CIIMAR - Interdisciplinary Centre of Marine and Environmental Research, Novo Edifício Do Terminal de Cruzeiros Do Porto de Leixões, Avenida General Norton de Matos S/N, 4450-208, Matosinhos, Portugal;
[4] *LAQV-REQUIMTE*, Department of Chemistry, University of Aveiro, 3810-193 Aveiro, Portugal

*Corresponding author email: vitor.hugo.oliveira@ua.pt
‡ Co-last authors

Abstract

An ongoing environmental restoration programme is using *Zostera noltii* transplants to rehabilitate metal(loid) contaminated habitats and enhance ecological health in a temperate coastal lagoon. However, the short-term effects of these interventions on resident benthic fauna remain poorly understood. In this study, mercury (Hg) bioaccumulation was assessed in the gills, hepatopancreas and gonads of the European green crab *Carcinus maenas*, along with temporal changes in Hg burdens and their influence on biochemical biomarker responses, at a historically contaminated site and a nearby reference site during the first two years following *Z. noltii* transplantation. At the contaminated site, all tissues exhibited higher Hg concentrations compared with the reference site, although differences were relatively low in magnitude. Notably, gonadal Hg decreased significantly from 2021 to 2022, highlighting the sensitivity of this organ to early habitat improvement. Biomarker responses were organ-specific: crabs from Laranjo Bay showed elevated antioxidant enzyme activities, such as catalase and glutathione-S-transferase, in the hepatopancreas, while gills experienced increased lipid peroxidation. Energy reserve mobilisation also varied across tissues, reflecting higher metabolic costs under contaminant exposure. Gonads maintained lower Hg levels and stable oxidative and energetic

profiles, highlighting their responsiveness as early indicators of environmental improvement. These findings reinforce the value of gonadal biomarkers for monitoring ecosystem recovery. Although *Z. noltii* expansion can promote metal(loid) phytostabilization and reduce contaminant bioavailability, the reductions in Hg accumulation observed in *C. maenas* after two years were limited, indicating an initial but still constrained ecotoxicological recovery of the estuarine ecosystem.

Keywords

Seagrasses; Oxidative stress; Energy budget; Rehabilitation; Nature-based Solutions (NbS)

1. Introduction

In recent decades, the intensification of human activities and industrial development in coastal areas, has led to significant environmental degradation. This phenomenon is especially evident in fragile ecosystems, such as estuaries, where the accumulation of contaminants, namely metal(loid)s, has caused profound alterations in the structure and functioning of natural habitats (Chakraborty et al., 2023; Kennish, 2002). Despite the implementation of several European directives aimed at the protection and recovery of aquatic ecosystems, such as the Water Framework Directive (Directive 2000/60/EC), the Habitats Directive (Directive 92/43/EEC), and the Marine Strategy Framework Directive (Directive 2008/56/EC), the effective remediation of historically contaminated areas remains a significant challenge.

A paradigmatic example of this issue is found in the Ria de Aveiro, a shallow coastal lagoon located in the central-northern region of Portugal. The Laranjo Bay, an inner basin of this lagoon, was severely impacted during the second half of the 20th century by the discharge of industrial effluents, mainly from the Estarreja Chemical Complex (Pereira et al., 1998). These effluents, rich in metal(loid)s such as mercury (Hg), arsenic (As), copper (Cu), cadmium (Cd), and lead (Pb) created a well-defined contamination gradient, with sediment concentrations that, some of them until recently, exceeded the Probable Effect Levels (PEL) set by the Canadian Interim Sediment Quality Guidelines (CCME, 2002), severely compromising local ecological health (Oliveira et al., 2025b, 2025c).

In this context, nature-based remediation strategies have been promoted, particularly bioremediation, an approach that employs living organisms to remove or neutralize contaminants (Pang et al., 2023; Singh et al., 2023). This method has gained attention due to its additional benefits, such as enhancing biodiversity and restoring ecological functions of habitats (Oliveira et al., 2024; Pang et al., 2023). In 2020, an ecological restoration approach was implemented in Laranjo Bay, based on the transplantation of the native seagrass *Zostera noltii*

(Oliveira et al., 2025a). This intervention enabled not only the structural recovery of the habitat but also supported biological recolonization and the re-establishment of local ecological interactions (Crespo et al., 2023). Moreover, *Z. noltii* has been shown to reduce the sedimentary bioavailability of Hg (Oliveira et al., 2023), which presents an advantage by limiting Hg accumulation in endobenthic organisms such as *Scrobicularia plana* and *Hediste diversicolor* (Oliveira et al., 2025b). However, the benefits of this restoration approach for the health of epibenthic fauna, such as *Carcinus maenas*, remain insufficiently explored. This species is a well-established bioindicator due to its tolerance to contaminated environments, its ecological significance within food webs, and its ability to bioaccumulate contaminants (Coelho et al., 2007; Pereira et al., 2006). These traits make it a suitable model for assessing the short-term effects of restoration interventions and for monitoring residual contamination levels in restored habitats. While conventional assessments typically focus on bioaccumulation, they can be strengthened by evaluating biological effects through biomarkers, such as biotransformation enzymes, energetic profile indicators, and oxidative stress profile (Hook et al., 2014), which reflect sub-organismal stress responses and provide sensitive early-warning signals (van der Oost et al., 2003).

Within this framework, the main objectives of this study were to evaluate temporal trends in total Hg concentrations in different tissues of *C. maenas* in areas with historical contamination; to assess the biochemical responses of *C. maenas* to Hg exposure, with emphasis on metabolic and antioxidant parameters; and to examine the impact of natural attenuation processes and ecological restoration interventions, such as *Z. noltii* transplantation, on reducing Hg bioavailability and mitigating its toxic effects in *C. maenas*.

2. Materials and methods

2.1. Study site description and sampling method

Carcinus maenas individuals were collected from two sites within the Ria de Aveiro (Portugal): a reference, non-contaminated site (near Cais do Bico) and a historically contaminated site (Laranjo Bay), as shown in Figure 1. Sediment analyses conducted by Oliveira et al. (2025b) confirmed a clear contamination gradient between the two locations. At Cais do Bico, sediment concentrations of metal(loid)s were relatively low, with values of Hg at 0.57 ± 0.01 mg Kg^{-1}, As at 18 ± 1 mg Kg^{-1}, Cd at 0.33 ± 0.04 mg Kg^{-1}, Cu at 15 ± 0 mg Kg^{-1}, and Pb at 21 ± 1 mg Kg^{-1}. In contrast, Laranjo Bay sediments showed significantly elevated concentrations: Hg at 9.1 ± 1.8 mg Kg^{-1}, As at 51 ± 5 mg Kg^{-1}, Cd at 0.82 ± 0.19 mg Kg^{-1}, Cu at 48 ± 11 mg Kg^{-1}, and Pb at 33 ± 4 mg Kg^{-1}. Sampling was conducted at two distinct time points: during the summer of 2021 (one year after the *Z. noltii* transplantation) and again in the summer of 2022 (two years post-

transplantation), with the aim of evaluating the temporal progression of the species' physiological and contaminant exposure status.

At each site, fifteen mature (stage 3) and similarly sized female *C. maenas* individuals were collected during low tide using baited circular drop nets. Selected crabs had cephalothorax widths ranging between 42 and 50 mm, corresponding to approximately 2+ year-old individuals (Coelho et al., 2008). Of these, ten individuals were used for biochemical analyses and five for Hg bioaccumulation assessments (only metal that significantly exceeds the Probable Effect Levels (PEL) set by the Canadian Interim Sediment Quality Guidelines (CCME, 2002)). Immediately after sampling, tissues (gills, hepatopancreas, and gonads) were removed, frozen in liquid nitrogen, and transported to the laboratory. At the laboratory, tissues for bioaccumulation analysis were stored at –20 °C, whereas for biochemical biomarkers were stored at –80 °C until further processing.

In parallel, water physicochemical parameters at each site (salinity, temperature, pH, and dissolved oxygen) were measured *in situ* during each sampling campaign.

2.2. Mercury quantification

To accurately determine the total Hg concentrations in gills, hepatopancreas, and gonads at each site, a LECO AMA-254 (Advanced Mercury Analyzer) was used, following the method described by Costley et al. (2000). Each sample was analysed in triplicate. Analytical precision was monitored using the certified reference material TORT-3 (Lobster hepatopancreas), with recovery rates ranging from 92% to 96% (n = 5), within the certified confidence interval. The coefficient variation among replicates was consistently below 10%.

2.3. Biochemical analysis

Gills, hepatopancreas, and gonads were divided into three aliquots (~25 mg fresh weight) to assess: (i) energy available, (ii) energy consumption, and (iii) biotransformation enzymes and oxidative stress profile (antioxidant defences and membrane damage).

To evaluate the energy available, tissues were homogenized at a 1:2 ratio in distilled water using a Potter–Elvehjem homogenizer. For the assessment of energy consumption, tissue aliquots were homogenized at a 1:5 ratio in 0.1M Tris-HCl pH 8.5 buffer with 15% (w/v) Poly Vinyl Pyrrolidone, 153 µM $MgSO_4$, and 0.2% (w/v) Triton X-100. The homogenates were centrifuged at 3000× g for 10 minutes at 4 °C, frozen in liquid nitrogen, and stored at –80 °C until the analysis of electron transport system activity.

Regarding the oxidative stress profile and biotransformation, tissues were homogenized at a 1:6 ratio in a chilled potassium phosphate buffer (0.1M, pH 7.4). Homogenates were divided into

two aliquots: one for lipid peroxidation (LPO) and another to obtain the post mitochondrial supernatant (PMS). For LPO, 100 µL of homogenate was stored with 10 µL of 4% butylatedhydroxytoluene and frozen in liquid nitrogen. The second aliquot was centrifuged at 12000× g for 20 minutes at 4 °C to obtain the PMS. Aliquots of PMS were prepared for the quantification of biotransformation enzymes (glutathione-S-transferases) and antioxidant profile (enzymatic: catalase, glutathione peroxidase, glutathione reductase; non-enzymatic antioxidants: total glutathione). For total glutathione determination, an additional PMS aliquot was prepared by precipitating the non-soluble PMS protein with 12% TCA (1:2 dilution). Briefly, PMS samples were incubated at 4 °C for 60 minutes, then centrifuged at 12000x g for 5 min at 4 °C. All PMS samples were immediately frozen in liquid nitrogen and stored at –80 °C until biochemical analyses were performed.

2.3.1. Energetic profile

Total lipids (LIP) were extracted following the Bligh and Dyer (1959) method. Briefly, chloroform and methanol were added to each sample, followed by centrifugation at 1000× g for 5 min. The organic phase was collected, treated with sulfuric acid, heated at 200 °C for 15 min, diluted with distilled water, and absorbance read at 370 nm using tripalmitin as the standard (Novais et al., 2013). For the quantification of total carbohydrate (CH) and proteins (PROT), samples were incubated in 15% TCA at –20 °C for 10 min and then centrifuged at 1000× g for 10 min. The supernatant was used for CH analysis, and the pellet for PROT determination. Total carbohydrates were determined using the phenol–sulfuric acid method, with 5% phenol and concentrated H_2SO_4, and measuring the absorbance at 492 nm using glucose as the standard. For PROT, pellets were resuspended in 1 N NaOH, incubated at 60 °C for 30 min, neutralized with HCl and measured at 592 nm following Bradford (1976) using bovine serum albumin as the standard. After analyses, LIP, CH and PROT were converted into energetic equivalents using established enthalpy combustion values: 39.5 kJ g^{-1} for LIP, 17.5 kJ g^{-1} for CH and 24 kJ g^{-1} for PROT (De Coen and Janssen, 2003, 1997). Results were expressed in millijoules (mJ) per milligram of fresh weight (F.W.). Energy consumption was estimated by measuring the activity of the electron transport system (ETS) activity, following the protocol of De Coen and Janssen (2003, 1997). This assay is based on the reduction of p-iodonitrotetrazolium (INT) to formazan. The reaction was monitored spectrophotometrically at 490 nm, with absorbance readings every 25 seconds over a 10-minute period at 20 °C. The concentration of formazan was calculated using an extinction coefficient (ε) of 15,900 M^{-1} cm^{-1}. ETS activity was converted into oxygen equivalents using the stoichiometric relationship: 2 µmol of formazan formed corresponds to 1 µmol of O_2 consumed (De Coen and Janssen, 1997). The amount of oxygen consumed was then

converted into energy equivalents using the specific oxygenthalpic value of 484 kJ mol^{-1} O_2 for a mixed substrate of LIP, PROT, and CH (Gnaiger, 1983). Results were expressed as mJ h^{-1} mg^{-1} of F.W.

2.3.2. Biotransformation and oxidative stress profile

The activity of the glutathione-S-transferase (GSTs) was assessed following Habig et al. (1974), using 1-chloro-2,4-dinitrobenzene (CDNB) as a substrate. Absorbance was registered at 340 nm every 30 seconds for 5 minutes and activity was expressed as nmol of GS-DNB formed min^{-1} mg^{-1} protein ($\varepsilon = 9.6 \times 10^3$ M^{-1} cm^{-1}). Catalase (CAT) activity was measured following the methodologies of Claiborne (1985) and Giri et al. (1996), based on the decomposition of hydrogen peroxide (H_2O_2). Absorbance was recorded at 240 nm every 10 seconds over 3 minutes at 25 °C. Activity was calculated using an $\varepsilon = 43.5$ M^{-1} cm^{-1} and expressed as µmol of H_2O_2 consumed min^{-1} mg^{-1} of protein. Glutathione peroxidase (GPx) activity was assessed according to the protocol of Mohandas et al. (1984), modified by Athar and Iqbal (1998), while glutathione reductase (GR) activity was determined following the method of Cribb et al. (1989). In both assays, the oxidation of NADPH was monitored at 340 nm every 30 seconds for 5 minutes at 25 °C. Enzymatic activity was expressed as nmol of $NADP^+$ formed min^{-1} mg^{-1} protein, using an $\varepsilon = 6.22 \times 10^3$ M^{-1} cm^{-1}. Total glutathione (GSHt) content was determined according to the methodology of Vandeputte et al. (1994). The formation of TNB resulting from this methodology is directly proportional to the sum of the concentrations of reduced glutathione (GSH) and oxidized glutathione (GSSG) present in the sample. The absorbance was read at 415 nm for 7 minutes at 30 seconds intervals at 25 °C. The formation of TNB concentration was expressed as nmol TNB conjugated min^{-1} mg^{-1} protein ($\varepsilon = 14.1 \times 103$ M^{-1} cm^{-1}). Lipid peroxidation was evaluated using the thiobarbituric acid reactive substances (TBARS) assay, as described by Bird and Draper (1984) and modified by Filho et al. (2001). TBARS levels, which reflect malondialdehyde (MDA) equivalents, were determined spectrophotometrically at 535 nm. MDA concentrations were calculated using an $\varepsilon = 1.56 \times 10^5$ M^{-1} cm^{-1} and expressed as nmol of TBARS formed mg^{-1} protein.

2.4. Statistical analysis

All data were statistically analysed using permutation multivariate analysis of variance (PERMANOVA). A two-way crossed design was applied, with Site (Cais do Bico and Laranjo Bay) and Time (1st and 2nd sampling campaigns) as fixed factors. Prior to the PERMANOVA, each factor was tested for its dispersion around the centroid using the PERMDISP analysis. All analyses were

performed using PRIMER v6 software with the PERMANOVA+ add-on (Anderson et al., 2008). Statistical significance was considered at $p \leq 0.05$.

3. Results

3.1. Site characterization

Environmental parameters were measured directly in the field (Table 1). Significant interaction effects between site and time factors were observed for salinity (F=608, p=0.001) and pH (F=184, p=0.001), with higher values recorded at Cais do Bico in 2021. Temperature showed a similar interaction effect (F=112, p=0.001), with higher values recorded in Laranjo Bay during summer 2021. For dissolved oxygen, expressed as a percentage of saturation, both site (F=133, p=0.001) and time (F=1113, p=0.001) were significant, with higher values recorded at Cais do Bico in 2022. In contrast, when dissolved oxygen was expressed in mg L^{-1}, significant differences were found only over time (F=49, p=0.001) with higher values observed in 2022 for both sites.

3.2. Total Hg accumulation in *Carcinus maenas*

Total Hg concentrations in the gills, hepatopancreas, and gonads of *C. maenas* (Table 2) showed distinct spatial and temporal patterns in 2021 and 2022. Significant differences between sites were observed in the gills (F=384, p=0.001) and hepatopancreas (F=261, p=0.001), with consistently higher Hg concentrations at Laranjo Bay compared to Cais do Bico. Despite this spatial contrast, Hg levels in these organs remained relatively stable between the two sampling years, and in both years the gills displayed higher Hg concentrations than the hepatopancreas, a result consistent with prior observations in 2003 (Table 2).

The gonads were the only organ to exhibit a significant interaction between site and sampling time (F=8.8, p=0.004). As observed for the other organs, gonads from Laranjo Bay consistently displayed higher Hg concentrations compared to those from Cais do Bico and specially in 2021 when concentration reached 0.76 mg Kg^{-1}. In 2022, concentrations in Laranjo Bay declined to 0.67 mg kg^{-1}, whereas values in Cais do Bico remained lower (Table 2).

3.3. Biochemical biomarker responses

3.3.1. Energetic profile

In the gills, the energetic profile showed significant differences between sites for CH (F=19, p=0.001), LIP (F=11, p=0.002), and ETS (F=4.6, p=0.043), while PROT levels did not differ significantly (Table 3). Carbohydrate content was higher at Cais do Bico compared to Laranjo Bay. In contrast, LIP content and ETS activity were higher at Laranjo Bay. Despite these differences, ETS activity in 2022 showed similar values between the two sites. In the

hepatopancreas, significant differences between sites were also observed for CH (F=12, p=0.001), LIP (F=11, p=0.005), and ETS (F=7.8, p=0.017), while PROT levels again did not show significant variation. Additionally, CH content varied significantly over time (Table 3; F=5.8, p=0.044). Both CH and LIP contents were higher at Cais do Bico than at Laranjo Bay. Moreover, CH levels were higher in 2022. Conversely, ETS activity was higher at Laranjo Bay in 2021. However, in 2022, ETS activity values were similar between the two sites. Regarding the energetic profile of the gonads (Table 3), no significant differences were observed between sites or sampling times.

3.3.2. Biotransformation and oxidative stress profile

In the gills (Figure 2), significant spatial differences were detected, with *C. maenas* collected from Laranjo Bay exhibiting higher CAT (F=38, p=0.001) and GPx (F=40, p=0.001) activities, as well as higher LPO levels (F=21, p=0.001) comparing to Cais do Bico. In contrast, the activities of GR (F=43, p=0.001), GST (F=367, p=0.001), and GSHt (F=1039, p=0.001) were lower at this site. Temporal differences were observed at Cais do Bico, where GPx activity (t=2.7, p=0.024) increased in the second campaign, while GST (t=3.5, p=0.001) and GSHt (t=12, p=0.001) activities decreased. At Laranjo Bay, only GSHt showed a slight reduction in activity during the second campaign compared to the first (t=4.6, p=0.001).

In the hepatopancreas (Figure 3), significant spatial differences were observed in the activity of CAT (F=99, p=0.001), GPx (F=42, p=0.001), GST (F=201, p=0.001), and GSHt (F=21, p=0.002), with higher values recorded at Laranjo Bay, except for GSHt, which displayed lower activity at this site. Regarding temporal variation, both GPx (t=2.4, p=0.046) and GST (t=4.2, p=0.017) exhibited significantly higher activities during the second campaign at Cais do Bico. However, at Laranjo Bay, GST activity decreased from the first to the second campaign (t=2.5, p=0.025). GR activity and LPO levels did not exhibit significant differences between sites or sampling times.

In the gonads (Figure 4), differences between sites were observed in CAT activity during the first campaign (t=4.1, p=0.005), GSHt in the second campaign (t=2.1, p=0.045), and GPx (F=22, p=0.002) and LPO (F=45, p=0.001) across both campaigns. Whenever significant differences were found, enzyme activities and LPO levels were consistently higher at Laranjo Bay. GR and GST activities showed no significant variation with respect to site or sampling time.

4. Discussion

4.1. Temporal trends of Total Hg in study sites and in *Carcinus maenas*

Total Hg concentrations in the surface sediments of the study areas have shown a consistent declining trend over time (Oliveira et al., 2025a, 2018). This reduction reflects a natural

attenuation processes, including the progressive deposition of cleaner sediments over historically contaminated layers and the cessation of industrial discharges since the late 20th century (M. E. Pereira et al., 2009). As a result, Hg levels in both surface sediments and suspended particles (Coelho et al., 2014) have diminished, reducing the exposure of benthic organisms and lowering the potential for bioaccumulation.

This environmental improvement is evident in the decreasing Hg body burdens of various bioindicator species, such as *S. plana* and *H. diversicolor* (Oliveira et al., 2025b). Similarly, temporal trends in *C. maenas* show a reduction in Hg concentrations at Cais do Bico, the site furthest from the primary contamination source, where significant decreases in both gills and hepatopancreas have been recorded since 1999 (Coelho et al., 2008, 2007; Pereira et al., 2006). At Laranjo Bay, however, the temporal decline is not yet statistically significant. Despite signs of sediment decontamination in this area (Castro et al., 2009; Rodrigues et al., 2010), surface sediment Hg concentrations remained relatively high in 2021, particularly in lower intertidal zones influenced by tidal erosion (9.1 ± 1.8 mg Kg^{-1}) (Oliveira et al., 2025b). In contrast, higher intertidal areas exhibited much lower concentrations (2.5 ± 0.2 mg Kg^{-1}) (Oliveira et al., 2025c). Given the spatial mobility of *C. maenas* across intertidal gradients, variability in sediment contamination may be buffered at the organism level, which could explain the lack of statistically significant differences in gill and hepatopancreas Hg concentrations between 2003 and 2021/2022. Furthermore, the similar Hg levels in these organs suggest a consistent organotropism pattern over time, reflecting their respective roles in uptake (gills) and detoxification (hepatopancreas). In contrast, the gonads, as a secondary storage organ, exhibited a declining trend in Hg levels between 2021 and 2022, indicating a more sensitive, organ-specific response potentially linked to lower long-term Hg burdens or physiological regulation during reproductive cycles.

The pattern described above underscores the importance of analysing multiple tissues when assessing environmental contamination and may reflect the early ecological benefits of *Z. noltii* restoration efforts initiated in 2020 in Laranjo Bay. Halophytes such as *Z. noltii* have been reported to enhance sediment quality by reducing sediment contaminant bioavailability (Oliveira et al., 2023), stabilizing sediments, and promoting the burial of contaminated layers, aided by local sedimentation rates (~0.7 cm/year) (Castro et al., 2009; Oliveira et al., 2018; Pereira et al., 1998). Such improvements have already been noted in other benthic species co-inhabiting the area, like *H. diversicolor* and *S. plana* (Oliveira et al., 2025b), indicating interspecific differences in metal uptake and sensitivity. However, the effects of restoration on Hg accumulation in *C. maenas* remain tissue-specific and subtle in the short-term. Notably, in 2024, spontaneous colonization of *Z. noltii* was recorded near the crab collection site (Oliveira

et al., 2025a), suggesting an adaptive response of the ecosystem to historical contamination. Over time, this natural expansion may strengthen phytostabilization processes, potentially leading to further declines in Hg bioaccumulation in *C. maenas*.

4.2. Biochemical status

Biochemical analyses provide sensitive and early-warning information on the physiological responses of *C. maenas* to environmental Hg exposure. Variations in energy metabolism and oxidative stress markers between organs, sites and sampling campaigns highlight organ-specific responses.

Energy reserve mobilisation differed clearly between tissues. In the gills of crabs from the contaminated Laranjo Bay, CH levels were consistently lower than at Cais do Bico, whereas LIP levels were higher. This divergence suggests that, despite increased contaminant exposure, LIP was not mobilised in the gills in the same way as CH. Several non-exclusive explanations are possible, such as Hg may inhibit local lipid catabolic enzymes, promote lipid accumulation associated with membrane remodelling or damage, or alter lipid transport between tissues (Bejaoui et al., 2025; Singaram et al., 2013), so that gill CH is used preferentially to support immediate metabolic needs while LIP remains relatively conserved or even accumulated locally. In contrast, in the hepatopancreas, both CH and LIP levels were significantly lower at Laranjo Bay, suggesting enhanced consumption of these reserves in response to Hg stress. This aligns with the hepatopancreas' recognised role as the main site of CH and LIP storage and mobilisation in crustaceans, including during the pubertal molt and other energetically demanding life stages (Li et al., 2022; Sánchez-Paz et al., 2006). Protein levels remained stable across sites and years in all organs, indicating that crustaceans tend to spare structural PROT under moderate stress, relying primarily on CH and LIP catabolism to sustain metabolism while preserving essential functions. Similar responses were reported by Arrigo et al. (2025), who showed that PROT degradation was only triggered under severe or prolonged stress (e.g. marine heatwaves).

The limited variation observed in gonadal energy reserves further supports the idea that reproductive tissues maintain energetic stability, as they rely largely on reserves accumulated earlier in the reproductive cycle (Li et al., 2022; Sánchez-Paz et al., 2007; Sugumar et al., 2013).

During the first sampling campaign, crabs from Laranjo Bay showed significantly higher ETS activity in both gills and hepatopancreas compared to Cais do Bico, indicating elevated metabolic turnover and increased ATP demand for stress responses (Herrera et al., 2024; Sokolova, 2018). Enhanced ETS may result in increased reactive oxygen species (ROS) formation, thus stimulating antioxidant defences. For example, Zhao et al. (2010) reported that low-level Hg exposure raised CAT and GPx activities in crabs. This is in line with the elevated CAT and GPx activities observed

at Laranjo Bay. Higher water temperatures recorded during the first campaign may also have contributed to these increases, as temperature is known to accelerate metabolic and enzymatic processes in crustaceans (Capparelli et al., 2019; Rodrigues et al., 2015).

During the second campaign, hepatopancreas LIP levels in Laranjo Bay remained lower than at Cais do Bico, showing no evidence of recovery of LIP stores. However, CH levels in this organ increased relative to the previous year, partly narrowing the difference between sites. This may reflect improved local conditions, such as higher food availability linked to *Z. noltii* expansion, or shifts associated with reproductive maturation, as CH demands fluctuate during oogenesis (Monteiro et al., 2025). In the gills, CH content remained stable between years at both sites, indicating that this reserve did not undergo further depletion during the second campaign. Throughout both years, gonadal CH, LIP, PROT and ETS showed no significant spatial or temporal variation, reinforcing the idea that reproductive tissues maintain energetic stability even when other organs experience metabolic adjustments (Li et al., 2022; Wang et al., 2014).

The observed oxidative stress profile was organ-specific. Gills were particularly sensitive, likely due to their direct exposure to contaminants and role in temporary metal storage (Ghedira et al., 2011; Laporte et al., 2002). Increased CAT and GPx activities with Hg concentration suggest an adaptive antioxidative response focused on peroxide detoxification. However, GST activity decreased in the more contaminated sites, consistent with findings by Maria et al. (2009). This decline may result from glutathione depletion due to its conjugation with Hg via sulfhydryl (-SH) groups (Ajsuvakova et al., 2020; Erofeeva, 2015; Sharma et al., 2012), forming less toxic GSH-Hg complexes, an adaptive strategy also seen in humans (Ajsuvakova et al., 2020; Endo and Sakata, 1995). Additionally, reductions in total GSH and GR activity in Laranjo Bay crabs suggest substantial GSH consumption without efficient regeneration. This antioxidant depletion is reflected in elevated LPO in gills, showing that a potential increase in ROS, possibly linked to elevated ETS activity, combined with reduced detoxification capacity resulted in membrane lipid damage. In the hepatopancreas, significant increase of CAT, GPx, and GST in contaminated site highlights the organ's robust antioxidant response to Hg exposure, corroborating findings from previous studies by Elumalai et al. (2007) and P. Pereira et al. (2009). This response reflects not only the efficiency of its antioxidant machinery but also the inherently high metabolic capacity of the hepatopancreas, which typically exhibits higher enzymatic activities and biochemical contents than the gills and gonads in both Cais do Bico and Laranjo Bay. The stable GR activity supports continuous GSH regeneration, although lower GSHt levels in Laranjo Bay point to its intensive use in detoxification. The absence of increased LPO further confirms the effectiveness of this antioxidant response in protecting lipid membranes. In contrast, the gonads showed generally low and stable antioxidant activity across sites and campaigns. Gonads from Laranjo

Bay exhibited higher LPO levels than those from Cais do Bico, and the slight increases in CAT and GPx observed at this site were not accompanied by changes in GR, GST, or GSHt. This relative stability may reflect several protective mechanisms: (i) the high LIP content of gonads, which can bind methylmercury and modulate its reactivity (Liu et al., 2018; O'Connor et al., 2019); (ii) the sequestration of Hg in non-reactive forms (e.g. bound to metallothioneins) in primary detoxification organs such as the gills and hepatopancreas (Kumar et al., 2025); and (iii) limited transfer of Hg to reproductive tissues. Additionally, because gonads were sampled during the reproductive season, when a substantial proportion of energy is channelled into reproduction (Dvoretsky et al., 2023; Griffen, 2018), these tissues may be more susceptible to oxidative disturbance, making any early improvements more detectable. The absence of temporal increases in oxidative damage or energetic disruption in the gonads may therefore represent an early and sensitive biological indication of improving environmental conditions, even if detoxifying organs continue to reflect legacy contamination.

Although clear biochemical improvements between 2021 and 2022 could not be demonstrated in most organs, the gonads were the only tissue in which Hg concentrations declined over this period (see Section 4.1). Despite Laranjo Bay showed higher LPO levels overall, oxidative damage did not increase from the first to the second campaign, and antioxidant activity remained stable. This temporal stability, combined with decreasing Hg burdens in the gonads, reinforce their sensitivity as an early tissue-specific signal of improving environmental conditions/ecosystem recovery. As environmental quality continues to improve, including contaminant phytostabilization and natural attenuation of the area, reductions in dissolved Hg concentrations, together with a diet consisting of less contaminated prey, may help decrease Hg bioaccumulation in the organs most directly exposed to metal(loid)s, progressively mitigating oxidative damage. Additionally, higher food availability could reduce the energetic costs of foraging, allowing more energy to be allocated to maintenance and detoxification processes. As previously highlighted, sampling occurred during the reproductive season, when a substantial proportion of energy is channelled into gonadal maturation, increasing physiological susceptibility to stress. This reproductive allocation may help explain why early signs of improvement were more readily detected in the gonads than in the detoxifying organs.

5. Conclusion

This study shows a clear decline in total Hg concentrations in *C. maenas* tissues, most notably in the gonads, reflecting the combined effects of natural attenuation, the cessation of industrial inputs and early benefits from *Z. noltii* restoration, which likely contributed to reduced Hg mobility and bioavailability. Improvements were more evident in Cais do Bico, but initial

recovery signals were also detectable in Laranjo Bay. Biochemical responses revealed organ-specific stress signatures, with gills and hepatopancreas sustaining the strongest detoxification demands and showing persistent evidence of legacy contamination. In contrast, gonads showed the earliest signs of improvement, emerging as sensitive indicators of better environmental quality, likely due to their limited detoxification capacity and higher physiological sensitivity during reproduction, making reductions in Hg burdens more readily detectable. Together, the geochemical and biological evidence suggests an initial yet promising trajectory of ecological recovery, with seagrass restoration and natural attenuation contributing to the gradual reduction of Hg exposure and its sublethal effects in *C. maenas*.

Declaration of Generative AI and AI-assisted technologies in the writing process

During the preparation of this work, the author(s) used ChatGPT to improve the language and readability of the manuscript. After using this tool/service, the author(s) reviewed and edited the content as needed and take(s) full responsibility for the content of the publication.

Declaration of competing interest

The authors declare that they have no known competing financial interests or personal relationships that could have appeared to influence the work reported in this paper.

Acknowledgements

The authors thank Sr. Aldiro Pereira for his invaluable help in the field work.

The authors acknowledge FCT – Foundation for Science and Technology for the PhD grant of Vitor Oliveira (reference 2020.04621.BD and DOI 10.54499/2020.04621.BD) and Ana Carvalhais (reference 2020.05105.BD and DOI 10.54499/2020.05105.BD) and the research contracts of João P. Coelho (reference 2020.01778.CEECIND/CP1589/CT0011 and DOI 10.54499/2020.01778.CEECIND/CP1589/CT0011), Marina Dolbeth (reference CEECINST/00027/2021/CP2789/CT0001 and DOI 10.54499/CEECINST/00027/2021/CP2789/CT0001), Ana I. Sousa (reference CEECIND/00962/2017/CP1459/CT0008 and DOI 10.54499/CEECIND/00962/2017/CP1459/CT0008), and Cláudia Mieiro (reference DL57/2016/CP1482/CT0028 and DOI 10.54499/DL57/2016/CP1482/CT0028).

This work was partially funded by project RemediGrass (PTDC/CTA-AMB/29647/2017) funded by FEDER, through COMPETE2020 - Programa Operacional Competitividade e Internacionalização (POCI), and by national funds (OE), through FCT/MCTES and Horizon Europe RESTORE4Cs project, funded by the European Commission (Grant agreement ID: 101056782;

10.3030/101056782). This work was also funded by national funds through FCT – Fundação para a Ciência e a Tecnologia I.P., under the project CESAM-Centro de Estudos do Ambiente e do Mar, references UID/50017/2025 (doi.org/10.54499/UID/50017/2025) and LA/P/0094/2020 (doi.org/10.54499/LA/P/0094/2020); and project CIIMAR-Centro Interdisciplinar de Investigação Marinha e Ambiental, references UID/04423/2025 (doi.org/10.54499/UID/04423/2025), UID/PRR/04423/2025 (doi.org/10.54499/UID/PRR/04423/2025), and LA/P/0101/2020 (doi.org/10.54499/LA/P/0101/2020).

6. References

Ajsuvakova, O.P., Tinkov, A.A., Aschner, M., Rocha, J.B.T., Michalke, B., Skalnaya, M.G., Skalny, A. V., Butnariu, M., Dadar, M., Sarac, I., Aaseth, J., Bjørklund, G., 2020. Sulfhydryl groups as targets of mercury toxicity. Coord. Chem. Rev. 417, 213343. https://doi.org/10.1016/j.ccr.2020.213343

Anderson, M., Gorley, R.N., Clarke, K., 2008. PERMANOVA+ for primer: Guide to software and statistical methods, Plymouth: Primer-E. https://learninghub.primer-e.com/books/permanova-for-primer-guide-to-software-and-statistical-methods.

Arrigo, F., Cunha, M., Vieira, H.C., Soares, A.M.V.M., Faggio, C., González-Pisani, X., Greco, L.L., Freitas, R., 2025. Impact of marine heatwaves on Carcinus maenas crabs: Physiological and biochemical mechanisms of thermal stress resilience. Mar. Environ. Res. 208, 107126. https://doi.org/10.1016/j.marenvres.2025.107126

Athar, M., 1998. Ferric nitrilotriacetate promotes N-diethylnitrosamine-induced renal tumorigenesis in the rat: implications for the involvement of oxidative stress. Carcinogenesis 19, 1133–1139. https://doi.org/10.1093/carcin/19.6.1133

Bejaoui, S., Chetoui, I., Ghribi, F., Belhassen, D., Trabelsi, W., Baati, R., Soudani, N., 2025. Mercury-induced lipid category disruption and Na+/K+-ATPase inhibition in Cerastoderma edule gills. Sci. Total Environ. 999, 180282. https://doi.org/10.1016/j.scitotenv.2025.180282

Bird, R.P., Draper, H.H., 1984. Comparative studies on different methods of malonaldehyde determination. pp. 299–305. https://doi.org/10.1016/S0076-6879(84)05038-2

Bligh, E.G., Dyer, W.J., 1959. A Rapid Method of Total Lipid Extraction and Purification. Can. J. Biochem. Physiol. 37, 911–917. https://doi.org/10.1139/o59-099

Bradford, M.M., 1976. A rapid and sensitive method for the quantitation of microgram quantities of protein utilizing the principle of protein-dye binding. Anal. Biochem. 72, 248–254. https://doi.org/10.1016/0003-2697(76)90527-3

Capparelli, M.V., Gusso-Choueri, P.K., Abessa, D.M. de S., McNamara, J.C., 2019. Seasonal environmental parameters influence biochemical responses of the fiddler crab Minuca rapax to contamination in situ. Comp. Biochem. Physiol. Part C Toxicol. Pharmacol. 216, 93–100. https://doi.org/10.1016/j.cbpc.2018.11.012

Castro, R., Pereira, S., Lima, A., Corticeiro, S., Válega, M., Pereira, E., Duarte, A., Figueira, E., 2009. Accumulation, distribution and cellular partitioning of mercury in several halophytes of a contaminated salt marsh. Chemosphere 76, 1348–1355. https://doi.org/10.1016/j.chemosphere.2009.06.033

CCME, 2002. Canadian sediment quality guidelines for the protection of aquatic life [WWW

498 Document]. URL https://ccme.ca/en/current-activities/canadian-environmental-quality-
499 guidelines (accessed 11.20.24).
500 Chakraborty, S.K., Sanyal, P., Ray, R., 2023. Pollution, Environmental Perturbation and
501 Consequent Loss of Wetlands, in: Wetlands Ecology. Springer International Publishing,
502 Cham, pp. 521–582. https://doi.org/10.1007/978-3-031-09253-4_8
503 Claiborne, A., 1985. Catalase activity, in: Handbook of Methods for Oxygen Radical Research.
504 CRC Press, Greenwald, pp. 283–284.
505 Coelho, J.P., Pato, P., Henriques, B., Picado, A., Lillebø, A.I., Dias, J.M., Duarte, A.C., Pereira,
506 M.E., Pardal, M.A., 2014. Long-term monitoring of a mercury contaminated estuary (Ria
507 de Aveiro, Portugal): the effect of weather events and management in mercury transport.
508 Hydrol. Process. 28, 352–360. https://doi.org/10.1002/hyp.9585
509 Coelho, J.P., Policarpo, E., Pardal, M.A., Millward, G.E., Pereira, M.E., Duarte, A.C., 2007.
510 Mercury contamination in invertebrate biota in a temperate coastal lagoon (Ria de
511 Aveiro, Portugal). Mar. Pollut. Bull. 54, 475–480.
512 https://doi.org/10.1016/j.marpolbul.2006.11.020
513 Coelho, J.P., Reis, A.T., Ventura, S., Pereira, M.E., Duarte, A.C., Pardal, M.A., 2008. Pattern and
514 pathways for mercury lifespan bioaccumulation in Carcinus maenas. Mar. Pollut. Bull. 56,
515 1104–1110. https://doi.org/10.1016/j.marpolbul.2008.03.020
516 Costley, C.T., Mossop, K.F., Dean, J.R., Garden, L.M., Marshall, J., Carroll, J., 2000.
517 Determination of mercury in environmental and biological samples using pyrolysis atomic
518 absorption spectrometry with gold amalgamation. Anal. Chim. Acta 405, 179–183.
519 https://doi.org/10.1016/S0003-2670(99)00742-4
520 Council Directive 92/43/EEC, 1992. Council Directive 92/43/EEC of 21 May 1992 on the
521 conservation of natural habitats and of wild fauna and flora. https://eur-
522 lex.europa.eu/eli/dir/1992/43/2013-07-01.
523 Crespo, D., Faião, R., Freitas, V., Oliveira, V.H., Sousa, A.I., Coelho, J.P., Dolbeth, M., 2023.
524 Using seagrass as a nature-based solution: Short-term effects of Zostera noltei transplant
525 in benthic communities of a European Atlantic coastal lagoon. Mar. Pollut. Bull. 197,
526 115762. https://doi.org/10.1016/j.marpolbul.2023.115762
527 Cribb, A.E., Leeder, J.S., Spielberg, S.P., 1989. Use of a microplate reader in an assay of
528 glutathione reductase using 5,5'-dithiobis(2-nitrobenzoic acid). Anal. Biochem. 183, 195–
529 196. https://doi.org/10.1016/0003-2697(89)90188-7
530 De Coen, W.M., Janssen, C.R., 2003. The missing biomarker link: Relationships between effects
531 on the cellular energy allocation biomarker of toxicant-stressed Daphnia magna and
532 corresponding population characteristics. Environ. Toxicol. Chem. 22, 1632–1641.

https://doi.org/10.1002/etc.5620220727
De Coen, W.M., Janssen, C.R., 1997. The use of biomarkers in Daphnia magna toxicity testing. IV. Cellular Energy Allocation: a new methodology to assess the energy budget of toxicant-stressed Daphnia populations. J. Aquat. Ecosyst. Stress Recover. 6, 43–55. https://doi.org/10.1023/A:1008228517955
Directive 2000/60/EC, 2000. Directive 2000/60/EC of the European Parliament and of the Council of 23 October 2000 establishing a framework for Community action in the field of water policy. https://eur-lex.europa.eu/eli/dir/2000/60/oj.
Directive 2008/56/EC, 2008. Directive 2008/56/EC of the European Parliament and of the Council of 17 June 2008 establishing a framework for community action in the field of marine environmental policy (Marine Strategy Framework Directive). http://data.europa.eu/eli/dir/2008/56/oj.
Dvoretsky, A.G., Bichkaeva, F.A., Baranova, N.F., Dvoretsky, V.G., 2023. Fatty Acid Profiles in the Gonads of Red King Crab (Paralithodes camtschaticus) from the Barents Sea. Animals 13, 336. https://doi.org/10.3390/ani13030336
Elumalai, M., Antunes, C., Guilhermino, L., 2007. Enzymatic biomarkers in the crab Carcinus maenas from the Minho River estuary (NW Portugal) exposed to zinc and mercury. Chemosphere 66, 1249–1255. https://doi.org/10.1016/j.chemosphere.2006.07.030
Endo, T., Sakata, M., 1995. Effects of Sulfhydryl Compounds on the Accumulation, Removal and Cytotoxicity of Inorganic Mercury by Primary Cultures of Rat Renal Cortical Epithelial Cells. Pharmacol. Toxicol. 76, 190–195. https://doi.org/10.1111/j.1600-0773.1995.tb00128.x
Erofeeva, E.A., 2015. Dependence of Guaiacol Peroxidase Activity and Lipid Peroxidation Rate in Drooping Birch (Betula pendula Roth) and Tillet (Tilia cordata Mill) Leaf on Motor Traffic Pollution Intensity. Dose-Response 13, 155932581558851. https://doi.org/10.1177/1559325815588510
Ghedira, J., Jebali, J., Banni, M., Chouba, L., Boussetta, H., López-Barea, J., Alhama, J., 2011. Use of oxidative stress biomarkers in Carcinus maenas to assess littoral zone contamination in Tunisia. Aquat. Biol. 14, 87–98. https://doi.org/10.3354/ab00377
Giri, U., Iqbal, M., Athar, M., 1996. Porphyrin-mediated photosensitization has a weak tumor promoting activity in mouse skin: possible role of in situ-generated reactive oxygen species. Carcinogenesis 17, 2023–2028. https://doi.org/10.1093/carcin/17.9.2023
Gnaiger, E., 1983. Calculation of Energetic and Biochemical Equivalents of Respiratory Oxygen Consumption, in: Polarographic Oxygen Sensors. Springer Berlin Heidelberg, Berlin, Heidelberg, pp. 337–345. https://doi.org/10.1007/978-3-642-81863-9_30

568 Griffen, B.D., 2018. The timing of energy allocation to reproduction in an important group of
569 marine consumers. PLoS One 13, e0199043.
570 https://doi.org/10.1371/journal.pone.0199043
571 Habig, W.H., Pabst, M.J., Jakoby, W.B., 1974. Glutathione S-Transferases. J. Biol. Chem. 249,
572 7130–7139. https://doi.org/10.1016/S0021-9258(19)42083-8
573 Herrera, I., de Carvalho-Souza, G.F., González-Ortegón, E., 2024. Physiological responses of the
574 invasive blue crabs Callinectes sapidus to salinity variations: Implications for adaptability
575 and invasive success. Comp. Biochem. Physiol. Part A Mol. Integr. Physiol. 297, 111709.
576 https://doi.org/10.1016/j.cbpa.2024.111709
577 Hook, S.E., Gallagher, E.P., Batley, G.E., 2014. The role of biomarkers in the assessment of
578 aquatic ecosystem health. Integr. Environ. Assess. Manag. 10, 327–341.
579 https://doi.org/10.1002/ieam.1530
580 Kennish, M.J., 2002. Environmental threats and environmental future of estuaries. Environ.
581 Conserv. 29, 78–107. https://doi.org/10.1017/S0376892902000061
582 Kumar, N., Priyadarshi, H., Parhi, J., Pandey, P.K., Kumar, D., 2025. Acute toxicity of mercury in
583 response to metallothionein expression and oxidative and cellular metabolic stress in
584 Barbonymus gonionotus. Sci. Rep. 15, 12022. https://doi.org/10.1038/s41598-025-
585 95697-1
586 Laporte, J., Truchot, J., Mesmer-Dudons, N., Boudou, A., 2002. Bioaccumulation of inorganic
587 and methylated mercury by the gills of the shore crab Carcinus maenas: transepithelial
588 fluxes and histochemical localization. Mar. Ecol. Prog. Ser. 231, 215–228.
589 https://doi.org/10.3354/meps231215
590 Li, W., Li, S., Wang, X., Chen, H., Hao, H., Wang, K.-J., 2022. Internal carbohydrates and lipids as
591 reserved energy supply in the pubertal molt of Scylla paramamosain. Aquaculture 549,
592 737736. https://doi.org/10.1016/j.aquaculture.2021.737736
593 Liu, M., Chen, L., He, Y., Baumann, Z., Mason, R.P., Shen, H., Yu, C., Zhang, W., Zhang, Q.,
594 Wang, X., 2018. Impacts of farmed fish consumption and food trade on methylmercury
595 exposure in China. Environ. Int. 120, 333–344.
596 https://doi.org/10.1016/j.envint.2018.08.017
597 Maria, V.L., Santos, M.A., Bebianno, M.J., 2009. Contaminant effects in shore crabs (Carcinus
598 maenas) from Ria Formosa Lagoon. Comp. Biochem. Physiol. Part C Toxicol. Pharmacol.
599 150, 196–208. https://doi.org/10.1016/j.cbpc.2009.04.013
600 Mohandas, J., Marshall, J.J., Duggin, G.G., Horvath, J.S., Tiller, D.J., 1984. Differential
601 distribution of glutathione and glutathione-related enzymes in rabbit kidney. Biochem.
602 Pharmacol. 33, 1801–1807. https://doi.org/10.1016/0006-2952(84)90353-8

603 Monteiro, J.N., Ovelheiro, A., Maia, F., Teodósio, M.A., Leitão, F., 2025. Biological traits and
604 population dynamics for sustainable harvesting of Carcinus maenas. Fish. Res. 281,
605 107243. https://doi.org/10.1016/j.fishres.2024.107243
606 Novais, S.C., Soares, A.M.V.M., De Coen, W., Amorim, M.J.B., 2013. Exposure of Enchytraeus
607 albidus to Cd and Zn – Changes in cellular energy allocation (CEA) and linkage to
608 transcriptional, enzymatic and reproductive effects. Chemosphere 90, 1305–1309.
609 https://doi.org/10.1016/j.chemosphere.2012.09.030
610 O'Connor, D., Hou, D., Ok, Y.S., Mulder, J., Duan, L., Wu, Q., Wang, S., Tack, F.M.G., Rinklebe, J.,
611 2019. Mercury speciation, transformation, and transportation in soils, atmospheric flux,
612 and implications for risk management: A critical review. Environ. Int. 126, 747–761.
613 https://doi.org/10.1016/j.envint.2019.03.019
614 Oliveira, V.H., Coelho, J.P., Reis, A.T., Vale, C., Bernardes, C., Pereira, M.E., 2018. Mobility
615 versus retention of mercury in bare and salt marsh sediments of a recovering coastal
616 lagoon (Ria de Aveiro, Portugal). Mar. Pollut. Bull. 135, 249–255.
617 https://doi.org/10.1016/j.marpolbul.2018.07.035
618 Oliveira, V.H., Díez, S., Dolbeth, M., Coelho, J.P., 2024. Restoration of degraded estuarine and
619 marine ecosystems: A systematic review of rehabilitation methods in Europe. J. Hazard.
620 Mater. 469, 133863. https://doi.org/10.1016/j.jhazmat.2024.133863
621 Oliveira, V.H., Fonte, B.A., Costa, F., Sousa, A.I., Henriques, B., Pereira, E., Dolbeth, M., Díez, S.,
622 Coelho, J.P., 2023. The effect of Zostera noltei recolonization on the sediment mercury
623 vertical profiles of a recovering coastal lagoon. Chemosphere 345, 140438.
624 https://doi.org/10.1016/j.chemosphere.2023.140438
625 Oliveira, V.H., Fonte, B.A., Sousa, A.I., Crespo, D., Dias, J.M., Vaz, N., Matos, D., Figueira, E.,
626 Pereira, M.E., Lillebø, A.I., Dolbeth, M., Coelho, J.P., 2025a. Transplantation of seagrass
627 (Zostera noltei) as a potential nature-based solution for the restoration of historically
628 contaminated mudflats. Sci. Total Environ. 959, 178257.
629 https://doi.org/10.1016/j.scitotenv.2024.178257
630 Oliveira, V.H., Marques, B., Carvalhais, A., Crespo, D., Dolbeth, M., Sousa, A.I., Lillebø, A.I.,
631 Pacheco, M., Pereira, M.E., Díez, S., Coelho, J.P., Mieiro, C.L., 2025b. Contaminant
632 bioaccumulation and biochemical responses of the bivalve Scrobicularia plana and the
633 polychaete Hediste diversicolor to ecosystem restoration measures using Zostera noltei.
634 Environ. Res. 275, 121429. https://doi.org/10.1016/j.envres.2025.121429
635 Oliveira, V.H., Matos, D., Sousa, A.I., Dolbeth, M., Marques, B., Lillebø, A.I., Pereira, M.E., Díez,
636 S., Figueira, E., Coelho, J.P., 2025c. Metabolic response of Zostera noltei transplants in a
637 historically contaminated ecosystem. J. Environ. Manage. 380, 124918.

https://doi.org/10.1016/j.jenvman.2025.124918
Pang, Y.L., Quek, Y.Y., Lim, S., Shuit, S.H., 2023. Review on Phytoremediation Potential of Floating Aquatic Plants for Heavy Metals: A Promising Approach. Sustainability 15, 1290. https://doi.org/10.3390/su15021290
Pereira, M.E., Abreu, S.N., Coelho, J.P., Lopes, C.B., Pardal, M.A., Vale, C., Duarte, A.C., 2006. Seasonal fluctuations of tissue mercury contents in the European shore crab Carcinus maenas from low and high contamination areas (Ria de Aveiro, Portugal). Mar. Pollut. Bull. 52, 1450–1457. https://doi.org/10.1016/j.marpolbul.2006.05.006
Pereira, M.E., Duarte, A.C., Millward, G.E., Abreu, S.N., Vale, C., 1998. An estimation of industrial mercury stored in sediments of a confined area of the Lagoon of Aveiro (Portugal). Water Sci. Technol. 37, 125–130. https://doi.org/10.1016/S0273-1223(98)00191-7
Pereira, M.E., Lillebø, A.I., Pato, P., Válega, M., Coelho, J.P., Lopes, C.B., Rodrigues, S., Cachada, A., Otero, M., Pardal, M.A., Duarte, A.C., 2009. Mercury pollution in Ria de Aveiro (Portugal): a review of the system assessment. Environ. Monit. Assess. 155, 39–49. https://doi.org/10.1007/s10661-008-0416-1
Pereira, P., de Pablo, H., Dulce Subida, M., Vale, C., Pacheco, M., 2009. Biochemical responses of the shore crab (Carcinus maenas) in a eutrophic and metal-contaminated coastal system (Óbidos lagoon, Portugal). Ecotoxicol. Environ. Saf. 72, 1471–1480. https://doi.org/10.1016/j.ecoenv.2008.12.012
Rodrigues, E.T., Moreno, A., Mendes, T., Palmeira, C., Pardal, M.Â., 2015. Biochemical and physiological responses of Carcinus maenas to temperature and the fungicide azoxystrobin. Chemosphere 132, 127–134. https://doi.org/10.1016/j.chemosphere.2015.03.011
Rodrigues, S.M., Henriques, B., Coimbra, J., da Silva, E.F., Pereira, M.E., Duarte, A.C., 2010. Water-soluble fraction of mercury, arsenic and other potentially toxic elements in highly contaminated sediments and soils. Chemosphere 78, 1301–1312. https://doi.org/https://doi.org/10.1016/j.chemosphere.2010.01.012
Sánchez-Paz, A., García-Carreño, F., Hernández-López, J., Muhlia-Almazán, A., Yepiz-Plascencia, G., 2007. Effect of short-term starvation on hepatopancreas and plasma energy reserves of the Pacific white shrimp (Litopenaeus vannamei). J. Exp. Mar. Bio. Ecol. 340, 184–193. https://doi.org/10.1016/j.jembe.2006.09.006
Sánchez-Paz, A., García-Carreño, F., Muhlia-Almazán, A., Peregrino-Uriarte, A.B., Hernández-López, J., Yepiz-Plascencia, G., 2006. Usage of energy reserves in crustaceans during starvation: Status and future directions. Insect Biochem. Mol. Biol. 36, 241–249.

https://doi.org/10.1016/j.ibmb.2006.01.002
Sharma, P., Jha, A.B., Dubey, R.S., Pessarakli, M., 2012. Reactive Oxygen Species, Oxidative Damage, and Antioxidative Defense Mechanism in Plants under Stressful Conditions. J. Bot. 2012, 1–26. https://doi.org/10.1155/2012/217037
Singaram, G., Harikrishnan, T., Chen, F.-Y., Bo, J., Giesy, J.P., 2013. Modulation of immune-associated parameters and antioxidant responses in the crab (Scylla serrata) exposed to mercury. Chemosphere 90, 917–928. https://doi.org/10.1016/j.chemosphere.2012.06.031
Singh, A.D., Khanna, K., Kour, J., Dhiman, S., Bhardwaj, T., Devi, K., Sharma, N., Kumar, P., Kapoor, N., Sharma, P., Arora, P., Sharma, A., Bhardwaj, R., 2023. Critical review on biogeochemical dynamics of mercury (Hg) and its abatement strategies. Chemosphere 319, 137917. https://doi.org/10.1016/j.chemosphere.2023.137917
Sokolova, I., 2018. Mitochondrial Adaptations to Variable Environments and Their Role in Animals' Stress Tolerance. Integr. Comp. Biol. 58, 519–531. https://doi.org/10.1093/icb/icy017
Sugumar, V., Vijayalakshmi, G., Saranya, K., 2013. Molt cycle related changes and effect of short term starvation on the biochemical constituents of the blue swimmer crab Portunus pelagicus. Saudi J. Biol. Sci. 20, 93–103. https://doi.org/10.1016/j.sjbs.2012.10.003
van der Oost, R., Beyer, J., Vermeulen, N.P.., 2003. Fish bioaccumulation and biomarkers in environmental risk assessment: a review. Environ. Toxicol. Pharmacol. 13, 57–149. https://doi.org/10.1016/S1382-6689(02)00126-6
Vandeputte, C., Guizon, I., Genestie-Denis, I., Vannier, B., Lorenzon, G., 1994. A microtiter plate assay for total glutathione and glutathione disulfide contents in cultured/isolated cells: performance study of a new miniaturized protocol. Cell Biol. Toxicol. 10, 415–421. https://doi.org/10.1007/BF00755791
Wang, W., Wu, X., Liu, Z., Zheng, H., Cheng, Y., 2014. Insights into Hepatopancreatic Functions for Nutrition Metabolism and Ovarian Development in the Crab Portunus trituberculatus: Gene Discovery in the Comparative Transcriptome of Different Hepatopancreas Stages. PLoS One 9, e84921. https://doi.org/10.1371/journal.pone.0084921
Wilhelm Filho, D., Tribess, T., Gáspari, C., Claudio, F.., Torres, M.., Magalhães, A.R.., 2001. Seasonal changes in antioxidant defenses of the digestive gland of the brown mussel (Perna perna). Aquaculture 203, 149–158. https://doi.org/10.1016/S0044-8486(01)00599-3
Zhao, Y., Wang, X., Qin, Y., Zheng, B., 2010. Mercury (Hg2+) effect on enzyme activities and

hepatopancreas histostructures of juvenile Chinese mitten crab Eriocheir sinensis. Chinese J. Oceanol. Limnol. 28, 427–434. https://doi.org/10.1007/s00343-010-9030-2

713 **Figure 1 -** Schematic map of the Aveiro Lagoon and Laranjo Bay (A), indicating the sampling
714 locations of *Carcinus maenas* near Cais do Bico (B) and in Laranjo Bay (C). Blue square indicates
715 the site of *Z. noltii* transplantation in 2020.
716

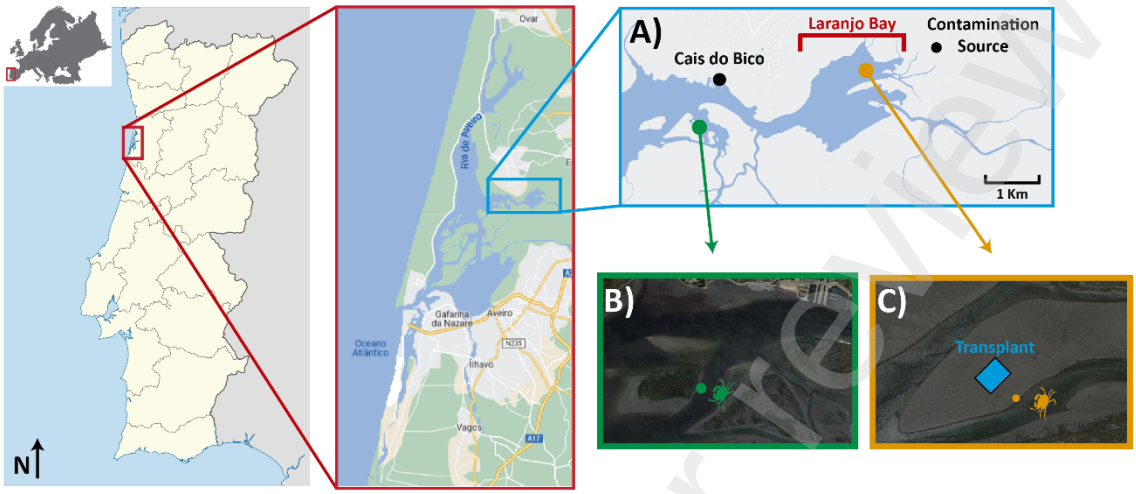

717
718
719

720 **Figure 2 –** Oxidative stress profile in gills of *Carcinus maenas* from Cais do Bico (CB) and Laranjo
721 Bay (LB) in 2021 and 2022. CAT: catalase; GPx: glutathione peroxidase; GR: glutathione
722 reductase; GST: glutathione-S-transferase; GSHt: total glutathione; LPO: lipid peroxidation.
723 Different superscript letters indicate significant differences ($p \leq 0.05$) between sites within the
724 same year. Asterisk (*) indicates significant differences between years at the same site.
725

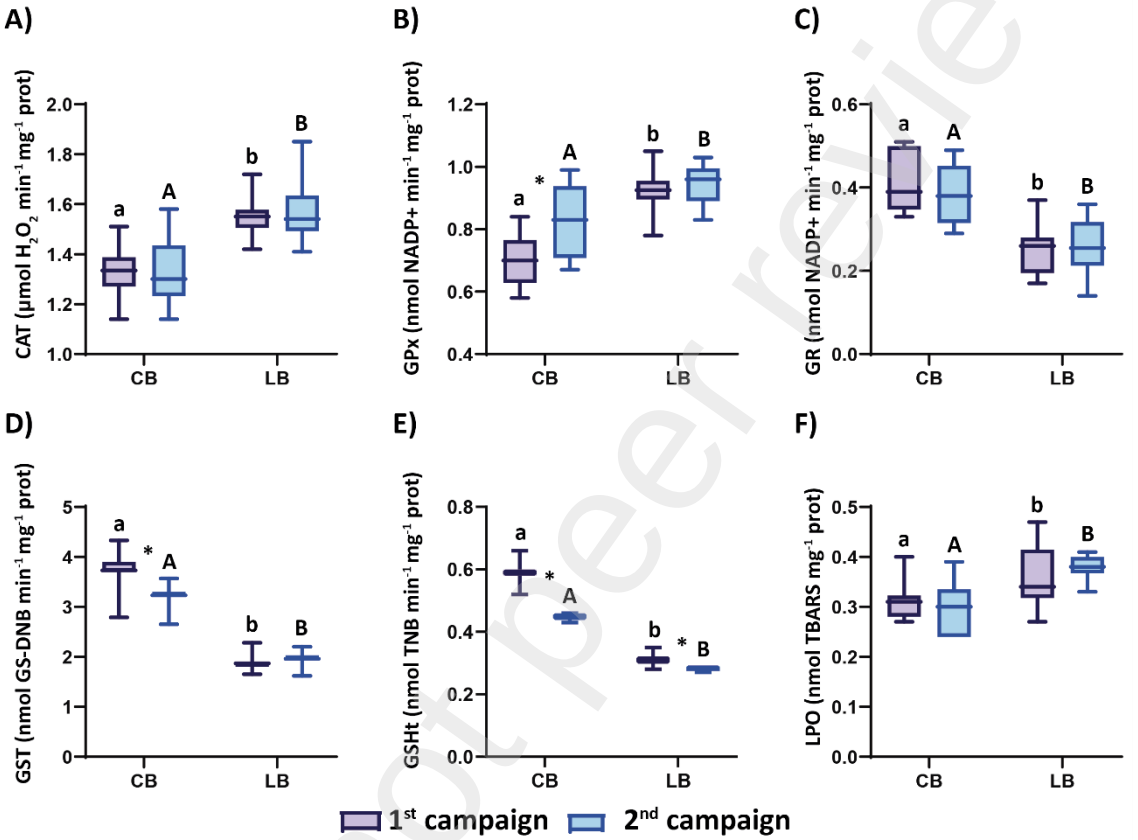

726
727
728

Figure 3 – Oxidative stress profile in the hepatopancreas of *Carcinus maenas* from Cais do Bico (CB) and Laranjo Bay (LB) in 2021 and 2022. CAT: catalase; GPx: glutathione peroxidase; GR: glutathione reductase; GST: glutathione-S-transferase; GSHt: total glutathione; LPO: lipid peroxidation. Different superscript letters indicate significant differences ($p \leq 0.05$) between sites within the same year. Asterisk (*) indicates significant differences between years at the same site.

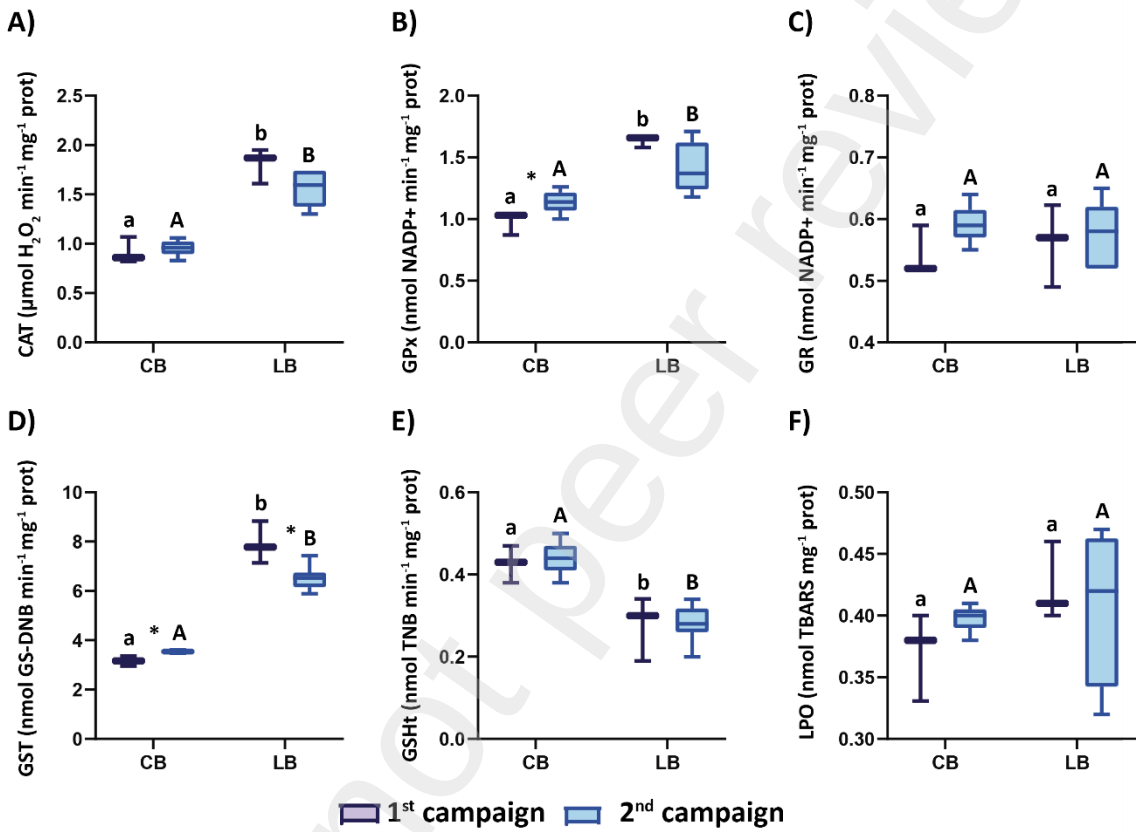

Figure 4 – Oxidative stress profile in the gonads of *Carcinus maenas* from Cais do Bico (CB) and Laranjo Bay (LB) in 2021 and 2022. CAT: catalase; GPx: glutathione peroxidase; GR: glutathione reductase; GST: glutathione-S-transferase; GSHt: total glutathione; LPO: lipid peroxidation. Different superscript letters indicate significant differences ($p \leq 0.05$) between sites within the same year. Asterisk (*) indicates significant differences between years at the same site.

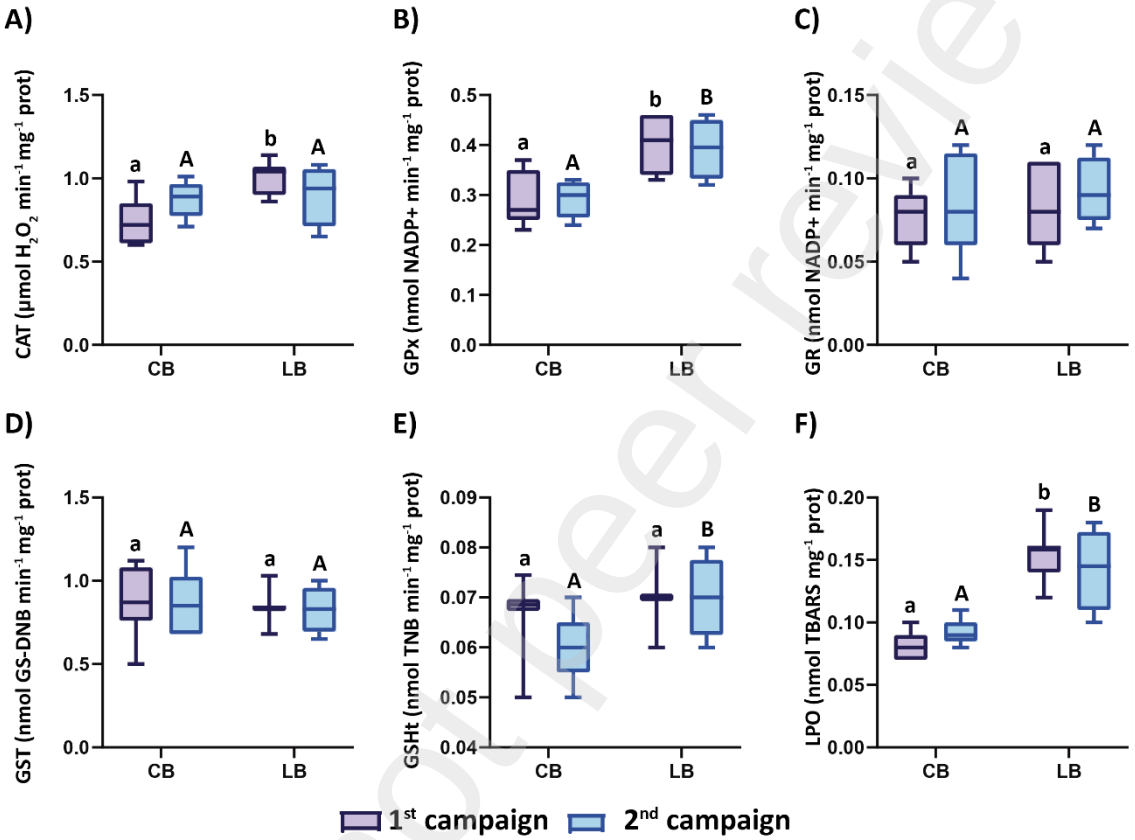

748 **Table 1 –** Physicochemical parameters (salinity, temperature, pH, and dissolved oxygen)
749 measured at Cais do Bico (CB) and Laranjo Bay (LB). Values are expressed as means ± standard
750 deviation. Different superscript letters denote statistically significant differences at the 95%
751 confidence level.
752

Time	Site	Salinity	Temperature (°C)	pH	O_2 (%)	O_2 (mg L^{-1})
2021	CB	30 ± 0 [(a)]	19 ± 0 [(a)]	7.8 ± 0.0 [(a)]	54 ± 1 [(a)]	5.0 ± 0.1 [(a)]
	LB	25 ± 0 [(b)]	21 ± 0 [(b)]	7.4 ± 0.0 [(b)]	47 ± 1 [(b)]	4.8 ± 0.7 [(a)]
2022	CB	31 ± 0 [(c)]	24 ± 0 [(c)]	7.7 ± 0.0 [(c)]	77 ± 3 [(c)]	6.3 ± 0.1 [(b)]
	LB	29 ± 0 [(d)]	24 ± 0 [(c)]	7.5 ± 0.0 [(d)]	68 ± 0 [(d)]	5.8 ± 0.1 [(c)]

753
754

Table 2 – Total mercury concentrations (mg Kg^{-1}) in the gills, hepatopancreas, and gonads of *Carcinus maenas* collected at Cais do Bico (CB) and Laranjo Bay (LB) over time. Values are presented as mean ± standard deviation. Different superscript letters indicate statistically significant differences between years at the 95% confidence level.

	Site:	**Year**			
		1999	**2003**	**2021**	**2022**
Gills	**CB**	0.92 ± 0.59 [(a)]	0.82 ± 0.03 [(a)]	0.49 ± 0.13 [(b)]	0.57 ± 0.09 [(b)]
	LB	---	1.5 ± 0.1 [(a)]	1.4 ± 0.2 [(a)]	1.4 ± 0.1 [(a)]
Hepatopancreas	**CB**	0.96 ± 0.63 [(a)]	0.63 ± 0.02 [(b)]	0.41 ± 0.17 [(c)]	0.37 ± 0.06 [(c)]
	LB	---	1.1 ± 0.1 [(a)]	0.95 ± 0.17 [(a)]	1.0 ± 0.1 [(a)]
Gonads	**CB**	---	---	0.21 ± 0.03 [(a)]	0.21 ± 0.01 [(a)]
	LB	---	---	0.76 ± 0.13 [(a)]	0.67 ± 0.04 [(b)]
Reference:		(Pereira et al., 2006)	(Coelho et al., 2008, 2007)	This study	

Table 3 – Energy budget parameters in gills, hepatopancreas, and gonads of *Carcinus maenas* in 2021 and 2022. PROT (protein), CH (carbohydrates), LIP (lipids): mJ mg^{-1} F.W.; ETS (Electron Transport System activity): mJ h^{-1} mg^{-1} F.W. Values are presented as mean ± standard deviation. Different superscript letters indicate statistically significant differences ($p \leq 0.05$) between sites (Cais do Bico (CB) and Laranjo Bay (LB)) within the same year. Asterisk (*) indicates a significant difference between years at the same site.

		Gills		Hepatopancreas		Gonads	
		2021	**2022**	**2021**	**2022**	**2021**	**2022**
PROT	**CB**	163 ± 19 $^{(a)}$	173 ± 19 $^{(a)}$	502 ± 31 $^{(a)}$	474 ± 47 $^{(a)}$	203 ± 26 $^{(a)}$	224 ± 16 $^{(a)}$
	LB	183 ± 37 $^{(a)}$	185 ± 33 $^{(a)}$	522 ± 35 $^{(a)}$	520 ± 64 $^{(a)}$	218 ± 29 $^{(a)}$	213 ±18 $^{(a)}$
CH	**CB**	53 ± 5 $^{(a)}$	52 ± 7 $^{(a)}$	115 ± 2 $^{(a)}$	122 ± 11 $^{(a)}$	58 ± 5 $^{(a)}$	53 ± 7 $^{(a)}$
	LB	42 ± 9 $^{(b)}$	42 ± 8 $^{(b)}$	86 ± 4 $^{(b)*}$	107 ± 15 $^{(a)*}$	60 ± 6 $^{(a)}$	50 ± 11 $^{(a)}$
LIP	**CB**	55 ± 9 $^{(a)}$	63 ± 21 $^{(a)}$	493 ± 22 $^{(a)}$	500 ± 33 $^{(a)}$	493 ± 55 $^{(a)}$	474 ± 56 $^{(a)}$
	LB	72 ± 15 $^{(b)}$	79 ± 13 $^{(a)}$	430 ± 10 $^{(b)}$	424 ± 49 $^{(b)}$	471 ± 37 $^{(a)}$	487 ± 29 $^{(a)}$
ETS	**CB**	5.9 ± 0.6 $^{(a)}$	6.5 ± 0.9 $^{(a)}$	11 ± 0 $^{(a)*}$	12 ± 0 $^{(a)*}$	5.2 ± 0.4 $^{(a)}$	6.0 ± 0.8 $^{(a)}$
	LB	6.8 ± 0.6 $^{(b)}$	6.7 ± 0.9 $^{(a)}$	13 ± 1 $^{(b)}$	12 ± 1 $^{(a)}$	5.0 ± 0.6 $^{(a)}$	5.0 ± 0.7 $^{(a)}$